Regional Scale Geothermal Field Development Optimization under Geological Uncertainties

S. Kahrobaei[1], R.M. Fonseca[1], C.J.L. Willems[2], F. Wilschut[1] and J.D. van Wees[1,3]

[1] TNO, Utrecht, The Netherlands

[2] University of Glasgow, Glasgow, United Kingdom

[3] Utrecht University, Utrecht, The Netherlands

siavash.kahrobaei@tno.nl

Keywords: Geothermal energy, optimization, production strategy, numerical simulations

ABSTRACT

In the geothermal energy domain, it is common practice to drill a doublet (i.e. an injection and production well pair) system for heat production from the subsurface. Injector-producer spacing typically varies between 1 to 2 km. This well spacing distance is usually chosen through engineering judgement. The concept of drilling doublet systems is a result of exploiting geothermal systems locally within a larger geological system. Willems (2017), illustrated through engineering judgement the need for improved well placement strategies. There exists significantly greater scope to optimize well placement strategies on a regional (i.e. geological system) scale, in view of optimizing the net energy gained.

Model based optimization of well location, trajectory and thereby spacing is common practice in the oil and gas industry. Additionally, due to the usually large uncertainty present in the subsurface it is essential to also account for geological uncertainties during optimization. In our framework, geological uncertainties are accounted for through an ensemble of equiprobable geological models. Thus, the goal is to find a single solution of well locations, which is optimal in terms of an expected objective function value over the ensemble of models. In this study we illustrate the added value of model based geothermal field development optimization at the regional scale in a positive trade-off with economic performance of single assets.

1. INTRODUCTION

In most real-world problems decisions are taken based on a model-based representation of the system. These models are traditionally used to predict the performance of the system. Based on these model predictions scenarios decision makers take investment and operational decisions. Most models make assumptions about the real system for a variety of reasons and many systems have inherent uncertainties associated with the modeling and physical aspects that describe the system. In addition to complex uncertainty these models depend on many decision variables. These decision variables, also known as controls, can have multiple values usually within a specified range. A collection of these decision variables is known as an operating strategy. In order to maximize the performance of the system using a model-based approach a decision maker aims to find an optimal operating strategy.

Finding an operating strategy is not trivial especially an operating strategy which comprises of many (100's-1000's) of decision variables (i.e. decisions on well location, well trajectory, material choices, ESP power, etc.). When uncertainty is accounted for the complexity of finding a strategy which is robust and optimal is very challenging. In this context, numerical optimization provides a viable solution to find robust and optimal operating strategies.

While there exist many optimization methods to find these optimal strategies most methods suffer from two drawbacks. One, the number of decision variables which the methods can handle is limited, usually, less than 100. Second, when accounting for uncertainty the methods are computationally not feasible even with recent advances in modern day computing architecture. In this work, a stochastic gradient approach, StoSAG (Fonseca et al. 2017), is employed for optimization. The main advantages of a stochastic gradient approach are its ability to effectively handle a large number of decision variables as well as model uncertainty in a very computationally efficient framework.

In the geothermal energy production domain, it is common practice to drill a doublet (i.e. a pair of injection and production wells) well system to produce hot water from the subsurface (Van Wees et al., 2012). This doublet pair is usually drilled 1-2 km apart (Lopez et al., 2010; Mottaghy et al., 2011). This well spacing distance is usually chosen through engineering judgement. Willems (2017) illustrated through relatively simple engineering analysis the need for improved well placement strategies. There potentially exists significantly greater scope to optimize well placement strategies on a regional (i.e. geological system) scale. The trajectory of these geothermal wells

is usually vertical and sometimes deviated. To maximize the energy production from geothermal systems it is imperative that a structured approach to life-cycle geothermal field development planning is developed. In this work we aim to illustrate the increased value achievable when using a model-based optimization technique to find optimal well location strategies when accounting for geological uncertainties.

The structure of this paper is as follows: a brief overview of the optimization method and the methodology to solve the optimization problem are provided in Section 2. The aquifer models used in this study are described in Section 3. Section 4 presents the results and discussions. Finally, we end the paper with some concluding remarks.

2. METHODOLOGY

Optimization is the process of finding the best possible solution for a particular problem. To optimize (i.e. find the best possible solution) any problem there must exist variables that can be manipulated/changed in order to achieve a better solution. These variables are known as *'Controls'*. Within the context of geothermal field development optimization these *'Controls'* can be defined as, well locations, trajectories, injection rates, well types, drilling schedule etc. Having defined the controls we aim to optimize, we must define a function to be optimized. Such a function is known as an *'objective function'* which in the context of geothermal field development optimization would be either an energy recovery factor or an economic objective.

An optimization process can either be manual or automated. Manual optimization is time consuming and prone to human bias and errors. Automated optimization on the other hand is quicker and less prone to human bias and errors. However the results from automated optimization workflows need to be analysed through human intervention. In the following section we describe a state-of-the-art automated workflow to perform optimization under uncertainty using computationally efficient techniques.

2.1. Stochastic Simplex Gradients (StoSAG)

There are numerous methods for model-based optimization. These methods can be classified into two general classes, derivative-based and derivative free techniques. Derivative/Gradient-based methods have been shown to be computationally more efficient than derivative free methods. In this work we employ a stochastic gradient based technique (StoSAG, (Fonseca et al., 2017)) as the optimization method which is described below.

2.1.1. Gradient Estimation Methodology

This section provides a diagrammatic representation of the StoSAG method for a single model realization. Imagine a two-control problem as displayed in **Figure 1**, where the controls are called $\mathbf{u}_1$ and $\mathbf{u}_2$. To approximate the gradient the following steps are undertaken.

- Chose an initial control strategy, e.g. the point [-1 0] in Figure 1.
- Generate a set of normally (Gaussian) distributed perturbed controls around the initial choice of $\mathbf{u}_1$ and $\mathbf{u}_2$. See the 'blue dots' in Figure 1.
- Evaluate the objective function values for each of the perturbed controls (blue dots). These are represented as the 'red dots' in Figure 1.
- Approximate the gradients by applying a linear regression through the red dots (green line in Figure 1).
- Use a simple line-search algorithm to find a new set of optimal controls in the direction of the gradient direction. This process is repeated till convergence (i.e. little/no change in the objective function) is observed.

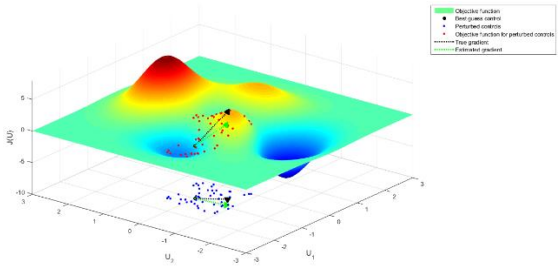

Figure 1: Schematic representation of the stochastic optimization technique for a simple two control problem.

In the case when uncertainty must be accounted for through the use of multiple model realizations we extend the use of the StoSAG method for such scenarios.

Chen (2008) suggested a computationally efficient technique to estimate the "robust ensemble gradient". Chen (2008) based on some assumptions suggested the use of one perturbed control sample for each model realization. Subsequently, the total number of simulations to estimate the "robust ensemble gradient" would be equal to the number of model realizations. This method is computationally attractive and can be applied to large scale optimization problems. Fonseca et al. (2017), introduced a theoretically more robust version of this formulation, StoSAG, which is used in this paper for the optimization.

2.2. Well Location Control Parameterization

Well grid block coordinates (i,j) are used as control variables to maximize the objective function by varying the well locations. Consequently, for vertical wells, which are assumed to be fully penetrating the aquifer model, this results in $2\times n_w$ controls where n_w is the number of wells. Thus, in a doublet system the control vector consists of four variables. Minimum and maximum number of grid blocks at each direction are used as the lower and upper bound constraints. Control variables and the bound constraints are scaled by the

maximum grid block number. Since the control parameter space is discrete, the updated control variables at each optimization iteration is rounded before passing to the simulator.

2.3. Objective Function

In this work we use an economic objective function, Net Present Value (NPV), which is developed by Van Wees et al. (2010). The NPV is discounted and consists of revenues generated by heat production and the associated costs for water injection as well drilling/workover costs. The produced energy at each time step, e_{prod} [J/s], is calculated as follows,

$$e_{prod,k} = q_i \rho_w C_w \Delta T_k, \quad [1]$$

where q_k [m^3/s] is the production rate and ΔT_k [K] is the difference between injection and production temperature at each time step k. ρ_w [kg/m^3] is the water density and C_w [J/kg K] is the specific heat capacity.

Moreover, the pressure difference between the injector and producer, Δp_k [Pa], is used to calculate the pump energy losses, e_{pump} [J/s], at each time step,

$$e_{pump,k} = \frac{q_i \Delta p_k}{\varepsilon}, \quad [2]$$

where ε [-] is the pump efficiency.

The net energy production is then calculated by the sum of the produced energy and the pump energy losses,

$$e_{net,k} = e_{prod,k} - e_{pump,k}. \quad [3]$$

Finally, the objective function (NPV) is calculated as follows,

$$J = \sum_{k=1}^{K} \left[\frac{(e_{net,k} \cdot r_h - e_{pump,k} \cdot r_e - CAPEX - OPEX_k)\Delta t_k}{(1+b)^{t_k}} \right], \quad [4]$$

where r_h [€/GJ] is the heat price, r_e [€/GJ] is the electricity cost for the operation. b is the discount rate and t_k is the time. CAPEX consists of costs for drilling, pumps and separators, which is invested at year 1. Moreover, OPEX is assumed to be 5% of CAPEX a year. **Table 1** represents the economic parameters for the objective function value calculations based on Van Wees et al. (2010) and Willems (2017).

Parameter	Value	Unit
Heat price	6	€/GJ
Electricity price for operations	22.22	€/GJ
Discount rate	7.5	%
Drilling cost	1.5	M€/km
Pump price	0.5	M€
Separator price	0.1	M€

Table 1: Economic parameters for the NPV calculations based on Van Wees et al. (2010) and Willems (2017).

3. GEOTHERMAL AQUIFER MODELS

Three different geothermal aquifer models have been used in this study. The Open Porous Media (OPM Flow) simulator has been used in this study for modelling non-isothermal flow through porous media. This section provides a description of the different models.

3.1. 2D Homogenous Model

A simple 2D homogenous with dimension of 5000 m × 5000 m with a thickness of 100 m has been used. The model is discretized in 100 × 100 grid blocks of size 50 m × 50 m. The aquifer has a constant permeability of 200 mD and porosity of 0.12. The initial reservoir temperature and pressure are assumed to be 65 ℃ and 50 bar, respectively. The rock and water thermal conductivity are 345.6 and 51.84 kJ/m/day/K, respectively. The heat capacities for the rock and water are 2.7 and 4.2 kJ/kg/K, respectively. The water has a density of 1000 kg/m3 and a viscosity of 0.001 Pa s. Note, these are the pure water properties at room temperature. Heat capacity and density for brine water composition would be different however will not significantly affect the result in terms of the proof of concept purpose of this study. The aquifer is produced with a single doublet with a well radius of 0.1778 m. The system (well) inputs are the (constant) water rate and water temperature in the injector and the (constant) water rate in the producer, which are all assumed to be known. Both injector and producer operate at a constant rate of 160 m^3/h, while the injector has a maximum pressure of 75 bar and the producer has a minimum pressure of 40 bar. The injection temperature is set to 35℃. The simulation life time is 100 years.

3.2. 2D Heterogenous Model

A channelized reservoir model has been used to study the effect of heterogeneity on well location optimization in geothermal heat production systems. The average permeability of the channels is 350 mD while the background shale facies has an average permeability of 20 mD and the aquifer has a constant porosity of 0.2. Other reservoir and fluid properties are the same as those used for the homogenous model. **Figure 2** illustrates the permeability and channel configuration used.

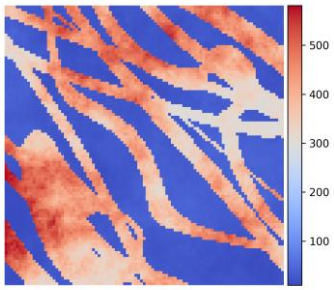

Figure 2: Permeability map of 2D heterogenous model.

3.3. 3D Regional Model

The aquifer realizations that have been used in the numerical production simulations are representations of the main geothermal aquifer target in the West Netherlands Basin. This target is part of the Late

Jurassic to Early Cretaceous Nieuwerkerk Formation (DeVault and Jeremiah, 2002). The aquifer target is characterized as a syn-rift, sandstone-rich interval of Valanginian age (Willems et al., 2018) within the Nieuwerkerk Formation. It was deposited in a in a coastal-plain setting. Stacked meandering sandstone-channel complexes form the aquifer, which are surrounded by impermeable floodplain fines. The geological modelling is based on a subsurface dataset described by Willems et al. (2017) and an outcrop study by Donselaar and Overeem (2008). Object-based modelling has been used to generate 100 aquifer realizations width dimensions of 5km × 5km × 150 m. The modeling is based on parameter values derived from descriptions of connected channel floor sandstones and point bar outcrops of the Huesca fluvial (Donselaar and Overeem, 2008). Figure 3 shows the permeability field of each layer in one of the models.

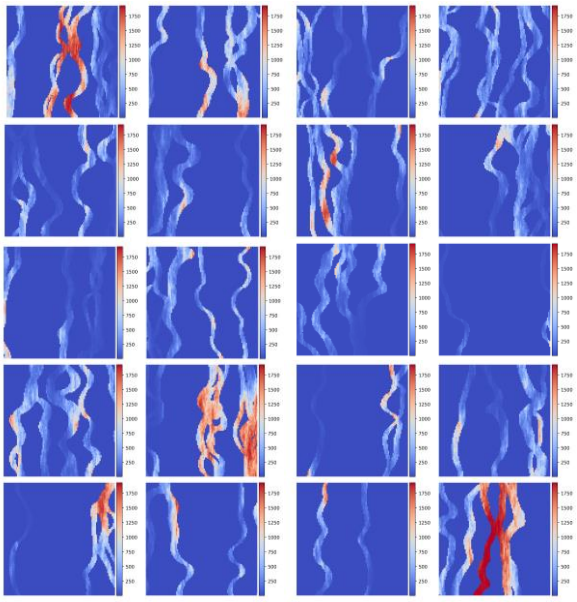

Figure 3: Permeability field of each layer in 3D model.

4. RESULTS AND DISCUSSION

A variety of optimization experiments have been performed using the different models to study the impact of different choices within the optimization framework. Optimization of well location and thereby well spacing is the focus of the optimization experiments in this study.

4.1. 2D Homogenous Case

The optimization workflow is set up for the 2D homogenous system, with an initial well spacing of 500 m. The standard deviation for control perturbation for gradient evaluations (perturbation size) is 0.03 with the number of perturbations being chosen to be 20 in this experiment. **Figure 4(a)** shows the production temperature during 100 years of production before and after optimization. **Figure 4(b)** is the objective function values (NPV) during 100 years of heat production, before and after optimization.

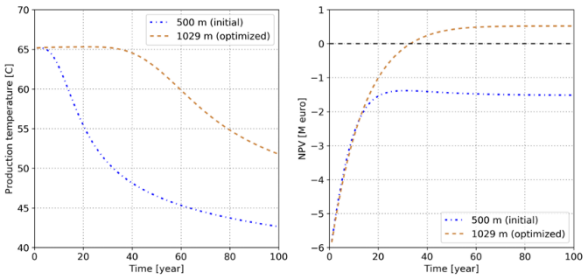

Figure 4: (a) Production temperature during 100 years of production before and after optimization. (b) Objective function value during 100 years of heat production before and after optimization.

Figure 4(a) reveals the heat breakthrough is delayed from year 2 to year 40 in the optimal strategy. This results in higher net energy production and subsequently objective function value increased from -1.5 M euro to 0.52 M euro. **Figure 5(a)** and **5(b)** show temperature map after 100 years of heat production with initial and optimized well locations, respectively. Blue and red dots represent the injector and the producer, respectively. After optimization the wells are located diagonally with a spacing of 1029 m. It is important to note that the wells are located in the center of grid blocks such that the exact distance of 1029 m cannot be achieved if the wells are located within the same row or column in the model**.** This explains why the wells are located diagonally in the optimal strategy.

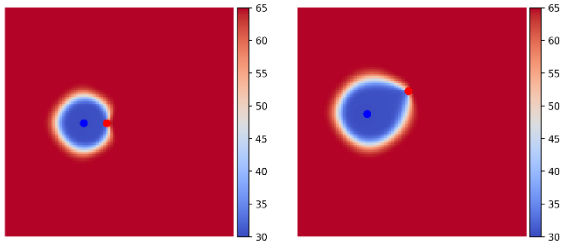

Figure 5: (a) Initial, (b) optimized temperature map after 100 years of production. . Blue and red dots represent the injector and the producer, respectively.

The stochastic nature of the optimization process implies the evaluation of a range of different well location configurations during the optimization iterations. Thus, many well spacing distances were evaluated which can be analyzed in the context of sensitivity analysis. Hence the sensitivity of the objective function to the well spacing can be observed in **Figure 6(a)**. **Figure 6(b)** magnifies the positive part of Figure 6(a)**.**

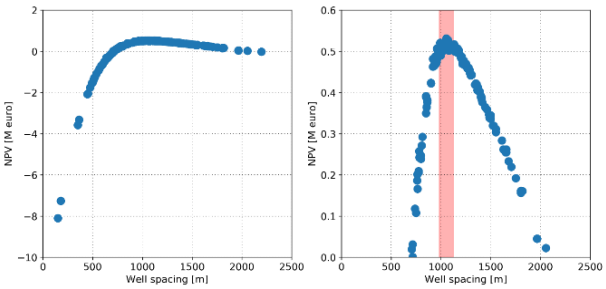

Figure 6: (a) NPV as a function of well spacing for a 2D homogenous system and (b) beneficial (positive) NPV as a function of well spacing for a 2D homogenous system. The red strip indicates the optimum region of the well spacing.

It can be seen from Figure 6 that the variations of the objective function value as a function of well spacing is not monotonic. The objective function value is initially increased as the well spacing increases up to an optimum well spacing above which the objective function value starts to decrease with further increases of the well spacing. Therefore, it can be concluded that there is a room for optimizing the well spacing in geothermal heat production systems, even for a simple 2D homogenous case with a single doublet.

4.2. 2D Heterogenous Case

The initial location of the injector well (blue dot) and producer wells (red dot) is illustrated in **Figure 7(a)**. The injector was initially placed in the shale and the producer was in the adjacent channel. **Figure 7(b)** is the simulated temperature map after 100 years of production.

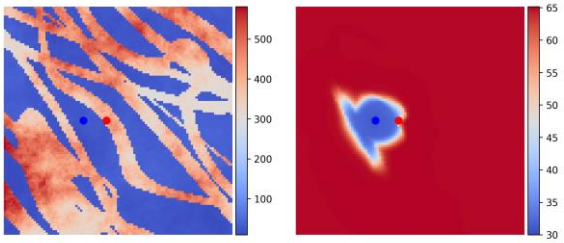

Figure 7: (a) Initial location of the injection (blue dot) and the production wells (red dot) on the permeability map. (b) Simulated temperature map after 100 years of production.

Figure 8 shows the well locations and the simulated temperature at year 100 after the optimization process.

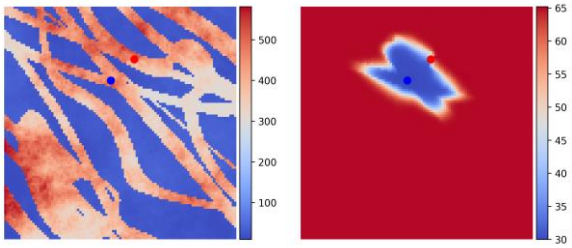

Figure 8: (a) Well locations and (b) simulated temperature at year 100 after optimization.

After the optimization process, both injection and production wells have been moved to the high permeable channels. It is important to note that the wells are in two different channels. Thus, the heat breakthrough is delayed quite significantly, while the injector provides the pressure supports to the producer through interconnected channels. This optimal strategy is non-trivial which highlights the importance of the optimization framework.

After the optimization the heat breakthrough is delayed since the wells are in two separate channels. On the other hand, the pressure drop is reduced significantly since the wells are still connected through the network of high-permeability channels. Consequently, higher production temperature and lower pressure drop increase the energy production and reduce the consumed energy. **Figure 9(a)** and **9(b)** show the produced and consumed energy respectively, before and after the optimization process.

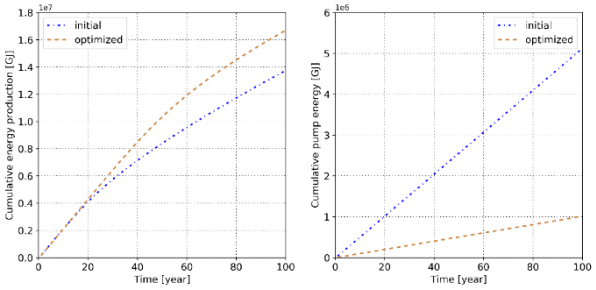

Figure 9: (a) Produced energy and (b) consumed energy by the pumps before and after the optimization process.

Finally, **Figure 10** shows the objective function evolution during 100 years of heat production before and after the optimization process. The NPV is increased from -14 million euro to 2.4 million euro after the optimization process.

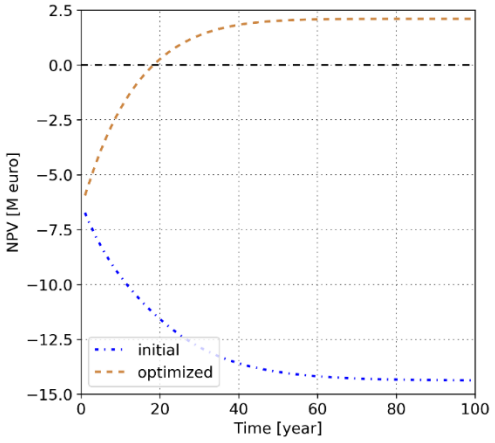

Figure 10: NPV during 100 years of heat production before and after optimization.

The same as the previous case, the optimization process involves large number of simulations with different sets of control combinations in the parameter space, which can be utilized to get more insights into the correlations

between the objective function and the control variables (well location).

Figure 11 shows the final NPV after 100 years of production as a function of well spacing extracted from the optimization workflow like the previous case. Figure 11 includes only the simulations, which have a positive NPV. Well spacing represents different combinations of injection and production locations. However, it is important to note that the well spacing is not a very good representative for well locations in a heterogenous system. In a heterogenous aquifer, well intersections with either sand bodies (high permeability medium) or shale (low permeability medium) is more influential than well spacing.

In contrast with a homogenous case, the points in Figure 11 are scattered all over the space. This is because the wells might have equal spacing but located in a high permeability channel or in low permeable shale. However, this indicates the importance of well placement optimization. The red dot in Figure 11 indicates the well spacing and its corresponded NPV after optimization process.

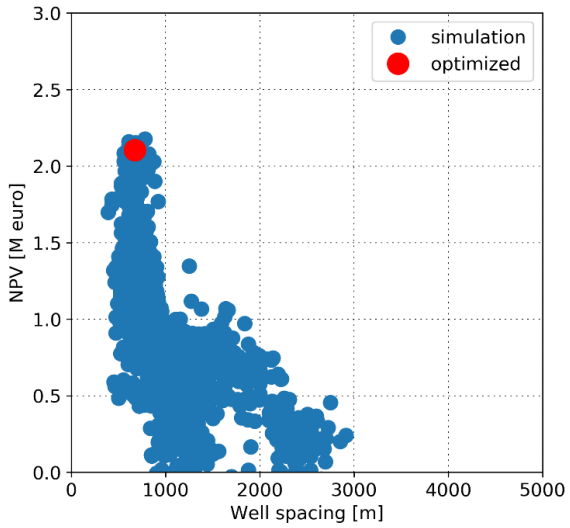

Figure 11: Beneficial (positive) NPV as a function of well spacing for a 2D heterogenous system. The red dot indicates the point, which is found in the optimization process.

4.3. 3D Regional Case

To investigate the potential value of regional scale geothermal field development within an optimization context a channelized 3D model, described in Section 3.3, has been employed. In this experiment, a multi-well system has been considered for efficient energy extraction from a much larger development area. Based on engineering judgement and accounting for the reservoir complexities a line drive production strategy with six wells was chosen as the initial development strategy (i.e., three doublet pairs). The well spacing between all doublets is chosen to be 2300 m initially. Since the model contains twenty layers it is almost impossible to find a vertical well trajectory, which will simultaneously intersect the high permeable channels in all layers. **Figure 12** is an illustration of this initial development strategy with well locations shown in six out of the twenty layers of the models. The figure also illustrates the corresponding simulated temperature after 100 years of production.

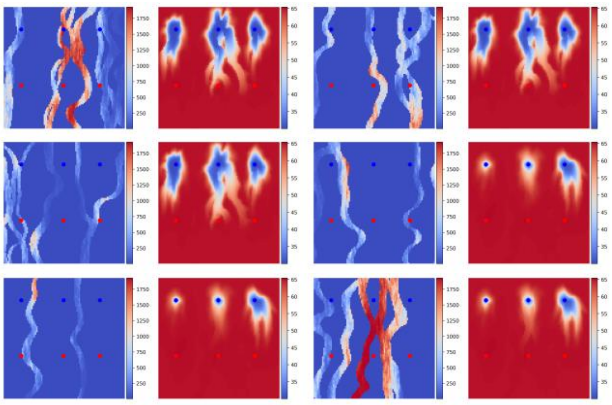

Figure 12: Initial well strategy and the corresponding simulated temperature after 100 years of production in first and last three layers of 3D model.

As can be seen in Figure 12, the well connectivity, especially in the last three layers, is poor as the production wells are located in areas with relatively poor reservoir quality which leads to low injection/production rates considering the maximum allowable injection pressure. This, albeit outside the scope of this paper, also points to the importance of well trajectory optimization to find deviated or horizontal well paths to intersect the best reservoir sections in all layers. **Figure 13** depicts the well locations and the corresponding temperature map in first and last three layers after the optimization process.

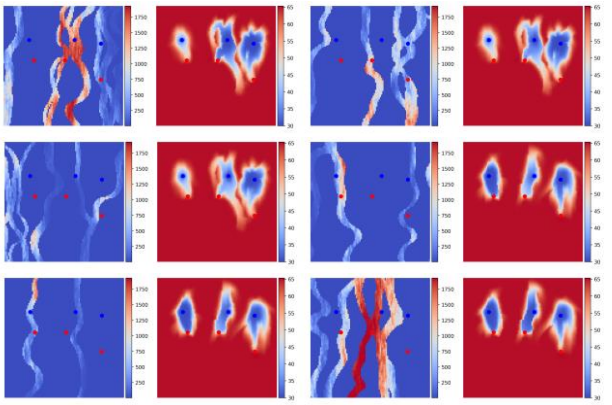

Figure 13: Optimized well strategy and the corresponding simulated temperature after 100 years of production in first and last three-layers of 3D model.

Although the well spacings were reduced after the optimization, the well connectivity improved significantly through the network of high-permeability channels. This results in achieving injection/production target rates. Subsequently, the energy production is increased because of an increase in the production rates. **Figure 14(a)** and **14(b)** show the injection and production rates before and after the optimization process. The injection/production rates in all wells reached the target rates after the optimization process.

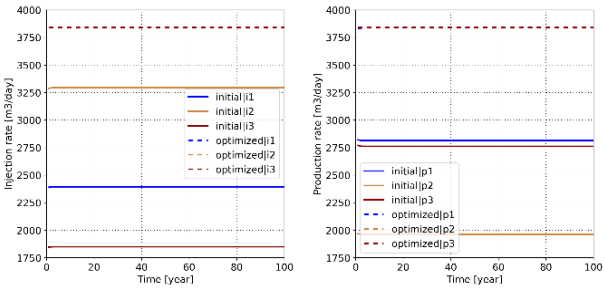

Figure 14: Injection and production rates before and after the optimization process.

Finally, **Figure 15** shows the objective function value during 100 years of heat production before and after the optimization process. The NPV is increased from -7 million euro to 5.3 million euro after the optimization process. Though this result might seem counter-intuitive from a well spacing perspective it highlights the value of model-based optimization workflows to find non-trivial solutions which are optimal on a regional scale considering the subsurface complexities.

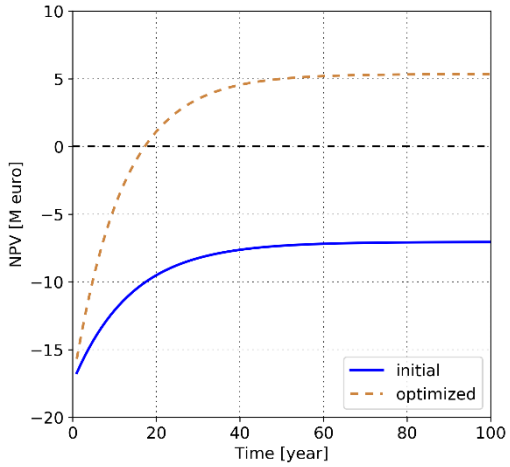

Figure 15: NPV during 100 years of heat production before and after optimization.

4.4. Optimization under Uncertainty

10 different homogenous permeability realizations have been used to capture the effect of geological uncertainty in well location optimization for geothermal heat production systems. The permeability of the realizations varied between 150 mD and 240 mD. Initial optimization results showed that despite significant variations in the well locations, the objective function values remained negative for the realizations with permeability values below 200 mD. A detailed analysis of these results led to a sensitivity analysis for a model with a permeability of 150 mD. **Figure 16** depicts the final NPV after 100 years of heat production from an aquifer with a permeability of 150 mD for a wide range of well spacings.

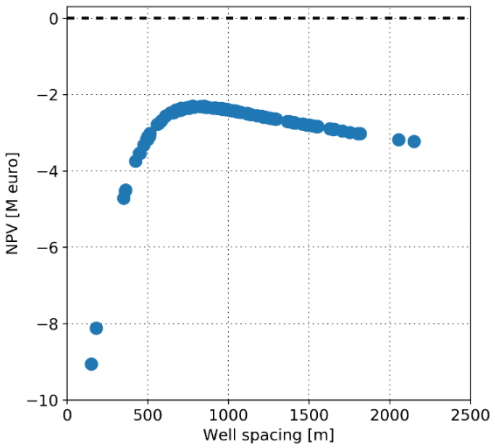

Figure 16: NPV as a function of well spacing for a 2D homogenous system with a permeability of 150 mD.

Figure 16 reveals that there exists no doublet location, which results in a positive NPV for this model with a permeability of 150 mD. In other words, because of its low permeability, if the wells become farther from each other, there is no sufficient pressure support to positively impact the economic objective function used in this paper. On the other hand, reducing the well spacing results in a very early heat breakthrough which reduces the amount of energy produced which again has a negative impact on the objective function. These two phenomena lead to there being no well spacing or location combination possible which would achieve a positive value of the objective function.

We observed that for a permeability of 200 mD or higher we were able to find optimal strategies which led to an expected positive objective function value. Therefore, for the robust optimization experiment an ensemble of 10 model realizations with permeabilities ranging between 200 and 290 mD were chosen to be optimized.

Figure 17(a) and **17 (b)** illustrate the evolution of the expected objective function value for the ensemble of model realizations for the initial and optimal strategy, respectively. The bold black solid line in both plots represents the expected objective function over the ensemble. The expected objective function with the initial well locations is -0.60338 million euros, which increased to 1.51 million euros after the optimization process. The optimal well locations were located at a well spacing of 1096 m compared to the initial strategy which had a spacing of 500m. The increase in the distance between the wells leads to a delay in the heat breakthrough for all the model realizations.

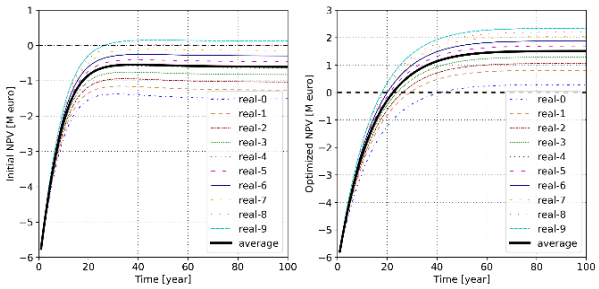

Figure 17: (a) NPV of 10 different model realizations before the optimization. The black solid line indicates the average NPV of the entire ensemble. (b) NPV of 10 different model realizations after the optimization. The black solid line indicates the average NPV of the entire ensemble.

These results are also in line with the results for the deterministic optimization explained the sections above. The optimal well locations achieved show only a difference of one grid block between the deterministic and robust experiments. This also highlights the value of incorporating uncertainty within an optimization workflow.

4. CONCLUSIONS

In this study we have shown the value of using numerical optimization techniques for well location optimization for a geothermal heat production system. The results show that non-trivial optimal solutions were obtained for three different cases with increasing model and development option scenarios. The importance of geological parameters and non-doublet systems were also highlighted by the results obtained in this study. The experiments were conducted with and without uncertainty in the model parameters. A semi-regional geological model was also constructed which is representative of the West Netherlands basin for a set of experiments on models which are more representative of real field cases. The results of these different types of experiments had common features which highlight the practical value of the optimization results.

REFERENCES

Chen, Y.: Efficient ensemble-based reservoir management, PhD Thesis, University of Oklahoma, (2008).

DeVault, B. & Jeremiah, J.L Tectonostratigraphy of the Nieuwerkerk Formation (Delfland Subgroup), West Netherlands Basin. *AAPG Bulletin*, (2002), 86(10), 1679–1707.

Donselaar, M.E. & Overeem, I.: Connectivity of fluvial point-bar deposits: an example from the Miocene Huesca fluvial fan, Ebro Basin, Spain. *AAPG Bulletin*, (2008), 92(9):1109–1129.

Fonseca, R. M.: A modified gradient formulation for ensemble optimization under geological uncertainty, PhD Thesis, Delft University of Technology, (2015).

Fonseca, R.M., Chen, B., Jansen, J. D., and Reynolds, A. (2017). A stochastic simplex approximate gradient (StoSAG) for optimization under uncertainty. *International Journal for Numerical Methods in Engineering.*

Lopez S., Hamm H., Le Brun M., Schaper L., Boissier, Cotiche C., Guiglaris, E.: 40 years of Dogger aquifer management in Ile-de-France, Paris Basin, France. *Geothermics (2010),39:339-356.*

Mottaghy, D., Pechnig. R., Vogt, C.: The geothermal project Den Haag: 3D numerical models for temperature prediction and reservoir simulation. *Geothermics (2011), 40:199-210.*

Van Wees, J.D, Kronimus, A., Van Putten, M., Pluymaekers, M., Mijnlieff, H., Van Hoof, P., Obdam, A. and Kramers, L.: Geothermal aquifer performance assessment for direct heat production – Methodology and application to Rotliegend aquifers, *Netherlands Journal of Geosciences*, (2012) 91-4, 651-665.

Willems, C.J.L., A. Vondrak, DK Munsterman, ME Donselaar, HF Mijnlieff: Regional geothermal aquifer architecture of the fluvial Lower Cretaceous Nieuwerkerk Formation–a palynological analysis. *Netherlands Journal of Geosciences*, (2018), 96 (4), 319-330.

Willems, C.J.L., Nick, H. M., Donselaar, M. E., Weltje, G. J., & Bruhn, D. F.: On the connectivity anisotropy in fluvial Hot Sedimentary Aquifers and its influence on geothermal doublet performance. *Geothermics*, (2017), 65, 222-233.

Williams, G.P.: River meanders and channel size. *J. Hydrol*. (1986), 88, 147 164.

Willems, C.: Doublet deployment strategies for geothermal hot sedimentary aquifer exploitation: Application to the lower cretaceous Nieuwekerk formation, west Netherlands basin, PhD Thesis, Delft University of Technology, (2017).